Structural Engineering and Mechanics, *Vol. 71, No. 2 (2019) 131-138*
DOI: https://doi.org/10.12989/sem.2019.71.2.131

Serviceability assessment of subway induced vibration of a frame structure using FEM

Yuhong Ling[1,4], Jingxin Gu[1], T.Y. Yang[2], Rui Liu*[3,4] and Yeming Huang[5]

[1]*Department of Civil Engineering and Transportation, South China University of Technology, Guangzhou 510640, China*
[2]*Department of Civil Engineering, The University of British Columbia, Vancouver, BC V6T 1Z4, Canada*
[3]*Architectural Design and Research Institute of SCUT, Guangzhou 510640, China*
[4]*State Key Laboratory of Subtropical Building Science, Guangzhou 510640, China*
[5]*Shum Yip Land Company Limited, Shenzhen 518040, China*

(Received January 14, 2019, Revised March 10, 2019, Accepted March 21, 2019)

Abstract. It is necessary to predict subway induced vibration if a new subway is to be built. To obtain the vibration response reliably, a three-dimensional (3D) FEM model, consisting of the tunnel, the soil, the subway load and the building above, is established in MIDAS GTS NX. For this study, it is a six-story frame structure built above line 3 of Guangzhou metro. The entire modeling process is described in detail, including the simplification of the carriage load and the determination of model parameters. Vibration measurements have been performed on the site of the building and the model is verified with the collected data. The predicted and measured vibration response are used together to assess vibration level due to the subway traffic in the building. The No.1 building can meet work and residence comfort requirement. This study demonstrates the applicability of the numerical train-tunnel-soil-structure model for the serviceability assessment of subway induced vibration and aims to provide practical references for engineering applications.

Keywords: frame structure; subway induced vibration; train-tunnel-soil-structure model; measurement; model parameters; serviceability assessment; one-third octave

1. Introduction

Subway brings us convenience and efficiency, but it can also cause some issues, such as affecting living quality and the safety of buildings built above. Therefore, it is necessary to solve those problem. With the coupling train-tunnel-soil-structure model based on MIDAS GTS NX, this study aims to study the simulation on vibration response of a six-story frame structure built above line 3 of Guangzhou metro, assess comfort requirement of the building and provide practical references for engineering applications.

Many researches have been conducted on prediction of subway induced vibration. The techniques range from classical mathematical analyses (Feng *et al.* 2017, He *et al.* 2019) to finite element (FEM) (dos Santos *et al.* 2017, Feng *et al.* 2017) and boundary element methods (BEM) (Jin *et al.* 2018, Yang *et al.* 2018). Obviously, complex models are computationally intensive (Connolly *et al.* 2015). For engineering practice, the balance adopted between accuracy and simplicity of the numerical approach proved to be a path to follow (Lopes *et al.* 2016). Lopez-Mendoza *et al.* (2017) set up a scoping model to predict railway induced vibrations which can be assessed in minimal computational time. Kuo *et al.* (2019) identified that simplified calculation models that do not include detailed railway structures can be adopted through the study of quantifying the coupling loss of buildings.

A common method for proving the reliability and accuracy of the numerical method proposed by the authors is to be compared with the measured vibration data. Bian *et al.* (2015) built a 2.5D vehicle-track-foundation coupled model, which has been validated using measurement data. Yang *et al.* (2015) conducted a vibration experiment on Chengdu museum and established a coupling tunnel-soil-structure finite element model to obtain the vibration characteristics of the museum caused by the subway. Kouroussis *et al.* (2016) built a prediction model validated against experimental data to discuss the main factors influencing the propagation of railway-induced ground vibration. Zou *et al.* (2015, 2017, 2018) verified the new 1D and 2D impedance model with the measured data for predicting vibration transmission in column and wall, concluding that axial propagation in the vertical direction dominates.

2. Numerical modelling

2.1 Problem outline

The No.1 building of the National Science Park of South China University of Technology is a scientific institute where the subway induced vibration may affect the application of precision instruments inside. It is a six-story frame structure with a total building height of 23.1 m. As

*Corresponding author, Senior Engineer
E-mail: liurui@scut.edu.cn

ISSN: 1225-4568 (Print), 1598-6217 (Online)

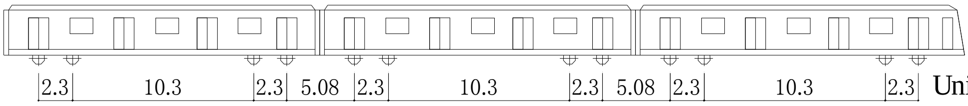

Fig. 3 Dimensions of three of the carriages

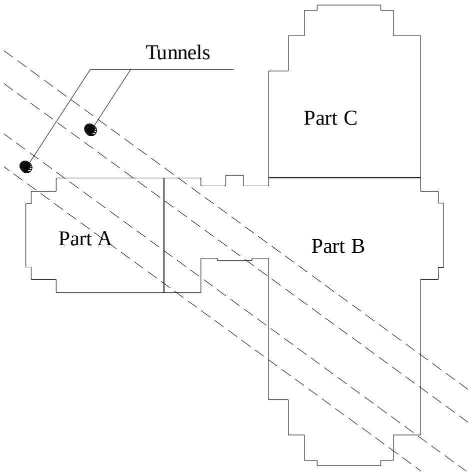

Fig. 1 Plane view of the No.1 building

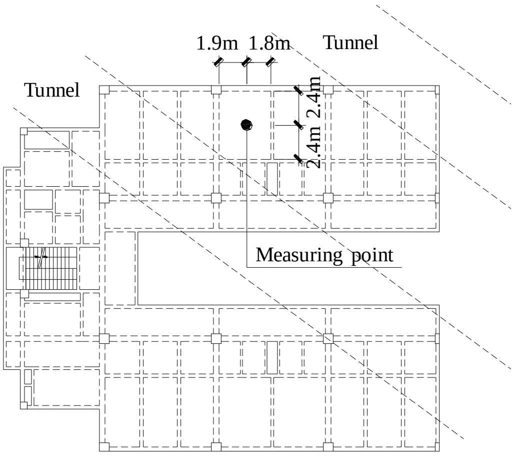

Fig. 2 Plane view of part A and layout of the measuring point

shown in Fig. 1, the building is divided into three parts by the construction joint. Part A (Fig. 2) is the research object in this paper which is directly built above line 3 of Guangzhou metro. In addition, neglecting the horizontal vibration, this study focuses on the vibration response in the vertical direction (the Chinese standard GB/T 50355-2005).

2.2 Train loading mode

Line 3 of Guangzhou metro has six carriages of the same size. The technical parameters of the train are shown in Table 1 and the dimensions of three of the carriages are shown in Fig. 3.

Each carriage is a vibration system with multiple freedom degrees. To facilitate the analysis, the following assumptions on the train-track model are used: a) The train body, bogie and wheels are regarded as rigid bodies and the elastic deformation is not considered. b) The transverse and vertical motions are not coupled so that the vertical vibration can be analyzed separately. c) The track is simplified as a continuous beam supported on a series of springs and it is meshed according to the sleeper spacing.

Table 1 Technical parameters of line 3 of Guangzhou metro

Length of train (m)	Width of train (m)	Height of train (m)	Distance of rail (m)	Distance of sleeper (m)
19.98	2.80	3.80	1.435	0.595
Fixed axle Spacing (m)	Maximum speed (m/s)	Average speed (m/s)	Axle load (kN)	
2.30	33.30	18.50	140	

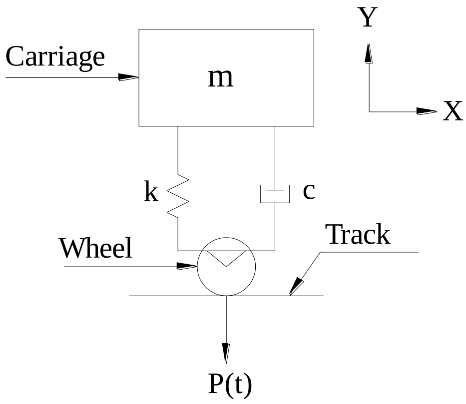

Fig. 4 Simplified model of the carriage

Fig. 4 shows the simplified model of vertical vibration of the carriage. The spring stiffness *k* and damping coefficient *c* are taken as 294 kN/cm and 50 kN•s/m. *P(t)* is the impact load. The equation of motion for the carriage is:

$$m\ddot{y} + c\dot{y} + ky + mg = 0 \tag{1}$$

$$P(t) + k\dot{y} + c\ddot{y} = 0 \tag{2}$$

$$P(t) = -k\dot{y} - c\ddot{y} = m\ddot{y} + mg \tag{3}$$

This paper adopts the Moving Axle Loads method (Auersch 2005) to calculate the train load, which assumes that the moving train applies a corresponding impact load when passing each node of the model, and ideally converts the impact load into a triangle. Fig. 5 shows the impact load of each moving wheel. In this paper, the average speed (18.5 m/s) is adopted, because the measuring point is located at the middle of two subway stations where the speed of the train is constant. The duration of the impact load on each node is approximately 6.5 s (19.98 * 6 / 18.5 = 6.5 s). In addition, the impact load is half of the axle weight (70 kN).

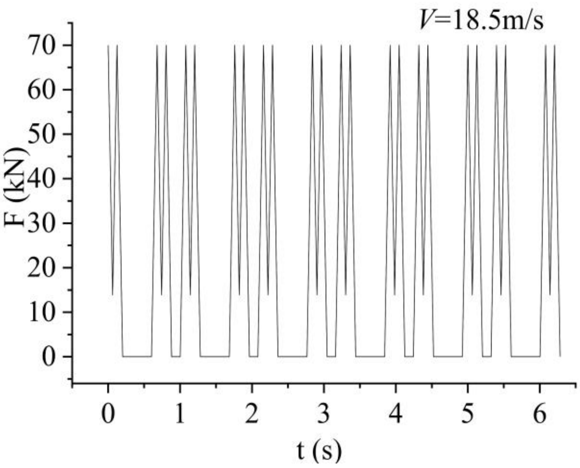

Fig. 5 Time history curve of the impact load

2.3 Damping ratio

Before dynamic analysis, eigenvalue analysis is needed to obtain the mode shapes and the corresponding periods. Analyzed through software, the eigenfrequency, corresponding to the vertical eigenmode, is 1 / 0.8569 = 1.167 Hz. Since there is a huge difference between the soil and the structure above, it is not suitable to simply take a value according to a substructure when determining the damping ratio of system. This paper applies the equivalent method proposed by Shibata and Sozen (1976). The idea is to separately obtain the potential energy of the soil and the structure, then multiply the respective damping ratios to obtain the damping ratio of system (Eq. (4)). In general, the damping ratio of concrete structure is 0.05 in the seismic analysis. However, in the vibration analysis where the energy level is much smaller than the earthquake, it becomes unreasonable. Considering the actual factors of this model, the damping ratio of structure is 0.01, the damping ratio of soil is 0.1, and the damping ratio of entire system is 0.03.

The damping ratio of system is:

$$\xi = \frac{\sum_{i=1}^{n} \xi_i W_i}{\sum_{i=1}^{n} W_i} \tag{4}$$

Where ξ is the damping ratio of system, ξ_i is the damping ratio of the ith structural member or the soil, W_i is the potential energy of the ith structural member or the soil.

Rayleigh damping method is adopted. Using the eigenfrequency corresponding to the first mode (1.167 Hz), and the eigenfrequency closest to the dominant frequency of the subway (50 Hz), with the identical damping ratio of system (0.03), the Rayleigh damping matrix (Eq. (5)) and the damping ratio at the center frequency of 1/3 octave can be obtained (Fig. 6).

The damping matrix is:

$$[C] = \alpha[M] + \beta[K] = 0.0684[M] + 1.1726\times10^{-3}[K] \tag{5}$$

Where $[C]$ is the damping matrix, $[M]$ is the mass matrix, $[K]$ is the stiffness matrix, α is the coefficient of mass proportional damping, β is the coefficient of stiffness proportion damping.

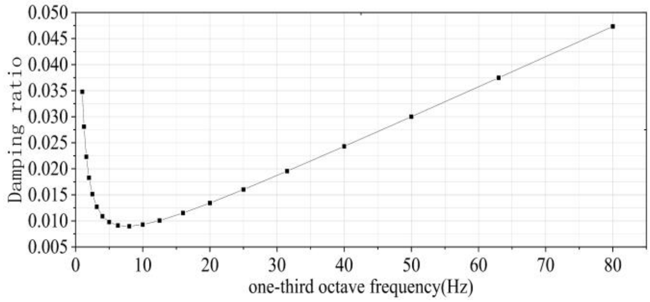

Fig. 6 The damping ratio at one-third octave frequency

Table 2 Reference material properties of the soil layers

Layer #	1	2-1	2-2	3
Thickness (m)	3.5	6.0	1.0	1.0
Density (kg/m^3)	1800	1910	1850	1920
Young's modulus (N/m^2)	10E6	15E6	20E6	15E6
Poisson ratio (dimensionless)	0.35	0.30	0.30	0.30
Damping ratio (dimensionless)	0.10	0.10	0.10	0.10
Layer #	4-1	4-2	5-1	5-2
Thickness (m)	3.0	9.0	9.0	8.0
Density (kg/m^3)	1900	1890	1970	2210
Young's modulus (N/m^2)	30E6	32E6	110E6	150E6
Poisson ratio (dimensionless)	0.30	0.28	0.25	0.22
Damping ratio (dimensionless)	0.10	0.10	0.10	0.10

2.4 Model of soil

At the site, two tunnels with an identical diameter of 6 m, are approximately 19 m below the ground (Fig. 7). The center distance between two tunnels is 15.2 m. The detailed soil parameters are shown in Table 2 which are obtained from the geotechnical investigation report as well as local experiment. Ideal elastic model is utilized to simulate the soil which follows the Mohr-Coulomb yield criterion.

For dynamic analysis, considering the interaction between soil and structure and selecting a reasonable range of the soil for the model are significant. At present, a wide-used method is to intercept the appropriate effective calculation region in the infinite domain and apply artificial boundary conditions in this region. The viscous boundary is suitable for analyzing the dynamic problem in elastic semi-infinite foundation, which can obtain good results with higher calculation efficiency (Lai *et al.* 2016). Hence, viscous boundary condition is applied to simulate an infinite foundation. According to engineering experience, vibration wave spreads effectively and evenly when the distance from the boundary of soil to tunnel wall is 2-5 times of the diameter of tunnel (6 m). To balance between efficiency and

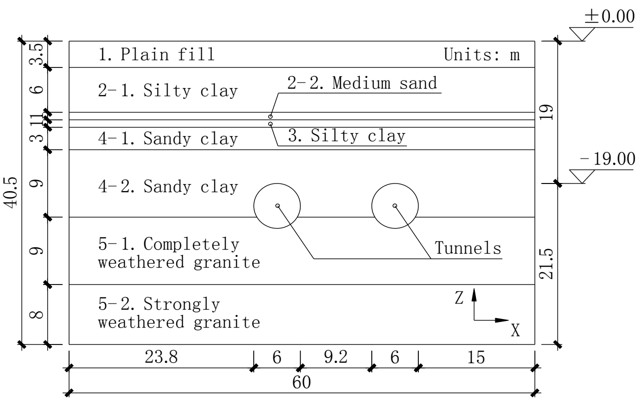

Fig. 7 Vertical position of the soil layers and the tunnels

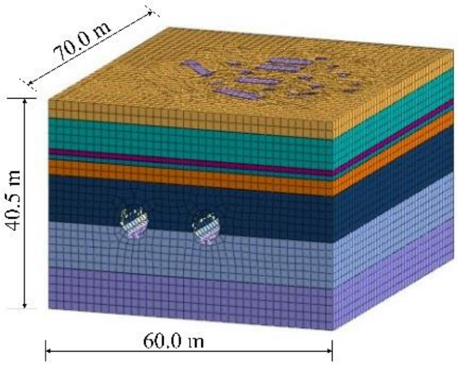

Fig. 8 Model of the soil

accuracy, the soil model is set up with a dimension of 70 m × 60 m × 40.5 m (Fig. 8).

2.5 Model of structure

The FEM model of the structure (Fig. 9) consists of lining segments, tubular piles, pile caps, columns, beams, floors and tracks. The parameters of the structural members are set as follows: the cross-sectional dimension of the frame columns is 600×600 mm, and the section of the constructional columns is 200×200 mm. The section of the frame beams is 400×700 mm, and the sections of the secondary beams are 250×600 mm, 200×500 mm, and 200×400 mm. The thickness of roof slab is 120 mm while the other slab is 110 m. The thickness of lining segments is taken as 300 mm, the diameter of tubular piles is 500 mm, and the thickness of tubular piles is 125 mm. The cross-section of the rails adopts the corresponding I-shaped steel of 60 kg/m. The rail can be considered as Euler beam since the span of the rail far exceeds the height of the beam. The shape and plane layout of the pile caps are shown in Fig. 10 which its thickness is 1.2 m or 2 m. The dead load including the structural self-weight and the superimposed dead load is taken as 1 kN/m^2. Live load of the slab is also taken as 1 kN/m^2 considering the actual load is not as high as the designed value. In addition, the beam load is added according to the different materials. The other parameters of structural members are shown in Table 3. The elastic constitutive relations are used to simulate materials.

Table 3 Parameters of the structural members

Structural member	Lining segment	Tubular pile	Pile cap
Material	C50 concrete	C80 concrete	C25 concrete
Element type	Shell element	Beam elemen	Solid element
Poisson ratio (dimensionless)	0.2	0.2	0.2
Damping ratio (dimensionless)	0.02	0.02	0.02
Young's modulus (N/m^2)	34.5E6	38E6	28E6

Structural member	Column	Beam	Floor	Track
Material	C30 concrete	C30 concrete	C30 concrete	Steel
Element type	Beam elemen	Beam elemen	Shell element	Beam elemen
Poisson ratio (dimensionless)	0.2	0.2	0.2	0.3
Damping ratio (dimensionless)	0.02	0.02	0.02	0.02
Young's modulus (N/m^2)	30E6	30E6	30E6	20.6E6

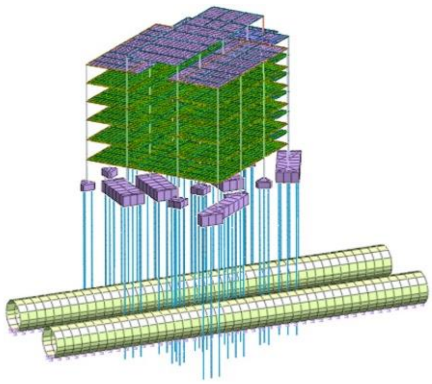

Fig. 9 Model of the structure

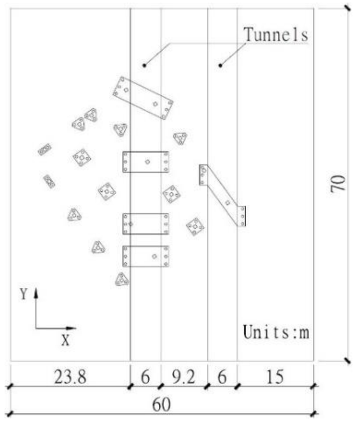

Fig. 10 Shape and plane layout of the pile cap

2.6 Model of system

The mesh size and the value of time step have a significant impact on the accuracy of calculation results. In this paper, the mesh size of structure is 1-1.5 m and the mesh size of soil is 1.5-2 m. As for the time step, according to Nyquist–Shannon sampling theorem, when the sampling

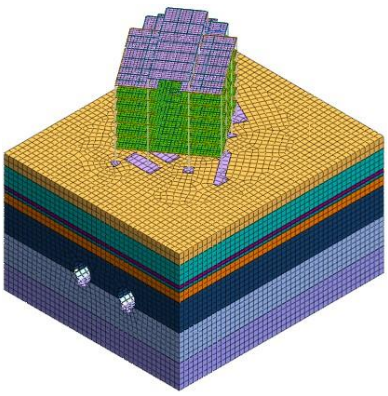

Fig. 11 Model of the system

frequency is greater than or equal to twice of the analysis frequency, the accuracy of engineering analysis can be met. The range of vibration frequency analyzed in this paper is between 0-80 Hz, that is, the time step should be less than or equal to the reciprocal of the frequency ($\Delta_t \leq 1/160 = 0.00625$ s). Thus, in this paper, the time step is 0.005 s whereas the total time is 10.48 s.

As for the contact problem between the soil and the superstructure, there are two common simulation methods: one is to consider the joint deformation between soil and structure by establishing the nodes shared by the two; the other is to simulate non-cooperative deformation between soil and structure by setting thin layer unit. It can be found that the amplitude of the first method is slightly 4 dB more than the second method. To be conservative, the first method is adopted. Similarly, for the coupling problem between the soil and the lining segments, in this study, the three translational degrees of freedom of them are coupled so that the contact can be considered. Fig. 11 shows the model of system developed by Midas GTS NX.

3. Vibration measurements

A series of measurements is carried out at a location in the part A. The national code (2005) stipulates that vibration measurement can be arranged with one measuring point placed in the center of indoor floor or in vibration sensitive areas. Therefore, sensors are arranged on each floor at the location shown in Fig. 2. The instrument used in the field measurement is the M series data acquisition which is developed by National Instruments. The supporting sensor is the LANCETEC's ULT20 series, with measuring range of ± 5 g, and resolution of 2×10^{-5} g. The conditional accuracy is in line with this measurement. Collecting data every 10 s, these measurements are made early in the morning between 06:30 and 07:30 when there is limited road traffic.

Through preliminary analysis, the vibration amplitude decreases with the increase of the floor when the vibration propagates in the frame structure, and the peak gradually decreases from 0.012 m/s^2 (the first layer) to 0.004 m/s^2 (the sixth floor). Moreover, it is found that the attenuation of vibration from the first layer to the second layer is larger. This is because the vibration of the second layer is propagated by the vertical members of the first layer which have a greater weakening effect on the vibration. The acceleration curves of each floor are similar in style and trend where the values are mainly concentrated in ± 0.003

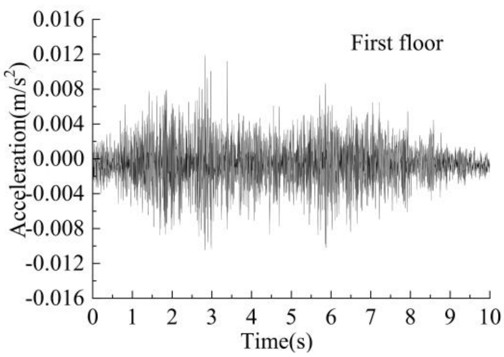

(a) First floor

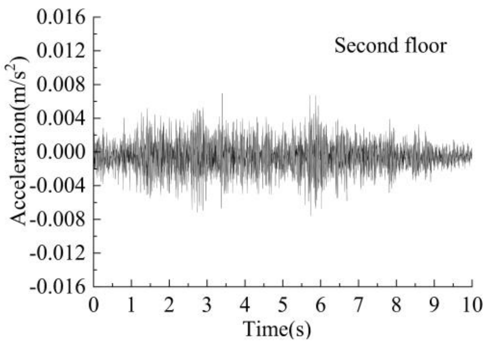

(b) Second floor

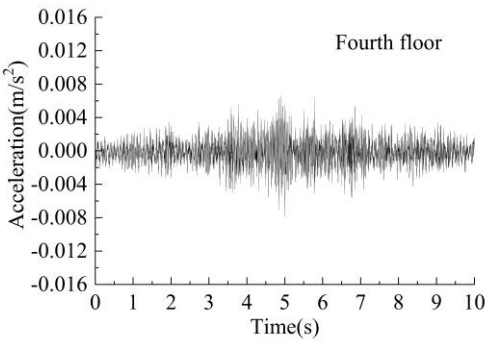

(c) Fourth floor

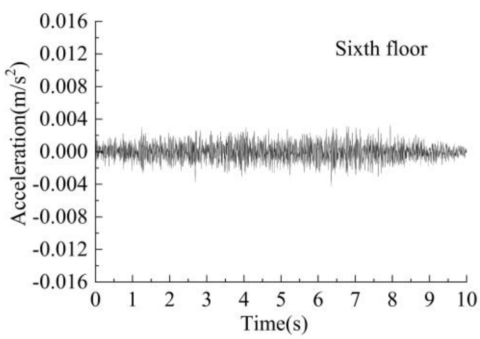

(d) Sixth floor

Fig. 12 Acceleration time history of the measuring point

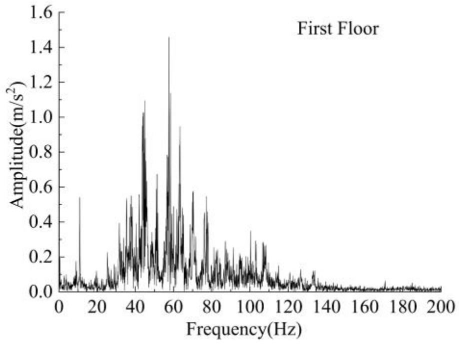

(a) First floor

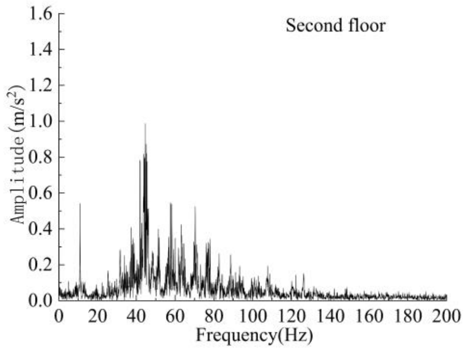

(b) Second floor

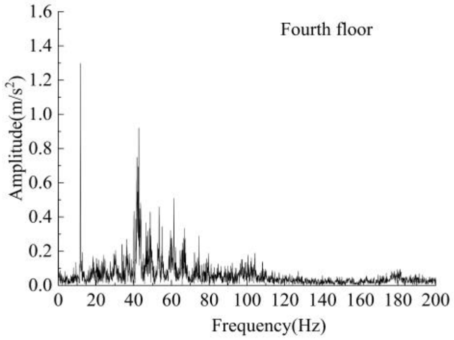

(c) Fourth floor

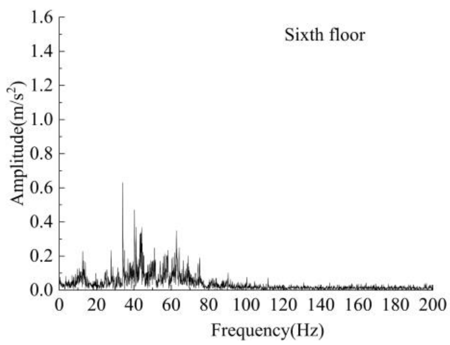

(d) Sixth floor

Fig. 13 Acceleration spectrum of the measured data

m/s^2. Occasionally there is a sudden change in acceleration, which is consistent with the randomness of vibration. Due to the limited space of the article, only the data of the first, the second, the fourth and the sixth layer are listed (see Fig. 12).

To study the vibration response of the corresponding frequency, it is necessary to perform Fourier transform.

Table 4 The central frequency of the one-third octave

Number #	1	2	3	4	5	6	7
Frequency (Hz)	1.0	1.25	1.6	2.0	2.5	3.15	4.0
Number #	8	9	10	11	12	13	14
Frequency (Hz)	5.0	6.3	8.0	10.0	12.5	16.0	20.0
Number #	15	16	17	18	19	20	
Frequency (Hz)	25.0	31.5	40.0	50.0	63.0	80.0	

That is, spectrum analysis, converting the time domain signal into the frequency domain spectrum on the evaluation amount of the vibration. The method adopted in this paper is one-third octave band. It can be seen from Fig. 13 that the frequency components of each floor are basically the same. The values are mainly concentrated at 30-80 Hz, which is similar to the previous research results (Ling *et al.* 2015, Li *et al.* 2016). The amplitude of the subway induced vibration mainly appears between 30-50 Hz. A sudden change in frequency at about 10 Hz. Inevitably, the measured data will be disturbed by ground vehicles (buses and cars) which its dominant frequency is 0-20 Hz.

4. Comparison and analysis

This part is to simulate and calculate the vibration response through the train-tunnel-soil-structure FEM model and compare it with the measured data on the vertical vibration acceleration level *VAL*. The *VAL* is shown with respect to the one third octave band. By doing so, it can evaluate structural comfort and verify the feasibility and correctness of the simulation method.

According to the national code (2005), vertical vibration acceleration level *VAL* corresponding to the one-third octave frequency (Table 4) can be used to evaluate the influence of vibration on human body.

Vibration acceleration level:

$$VAL=20\ lg\frac{a}{a_0}\quad (dB) \tag{6}$$

Where a is effective value of vertical vibration acceleration, $a=\sqrt{\frac{1}{T}\int_0^T a_i^2(t)\,d(t)}$ (m/s^2); a_0 is reference acceleration, $a_0=10^{-6}\ m/s^2$.

The analysis results are shown in Fig. 14. By comparing measured result and model result, it is seen that both of them are similar in the vibration acceleration level at the central frequency of the one-third octave. As the frequency increases, the vibration level first increases (1-40 Hz) and then decreases (40-80 Hz), and the maximum value (64 dB) occurs around 40 Hz. However, in the range of 1-4 Hz and 50-80 Hz, the model result is smaller than the measured result. But the accuracy is satisfactory for engineering applications. In the sensitive range of human body (4-30 Hz) and the main frequency of the subway induced vibration (30-50 Hz), the curves of the two are quite close. In addition, by comparing the vibration response with the

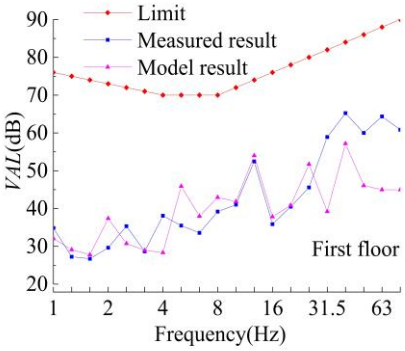

(a) First floor

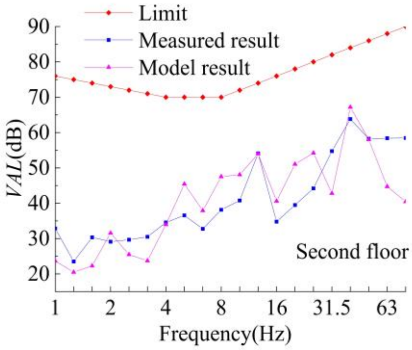

(b) Second floor

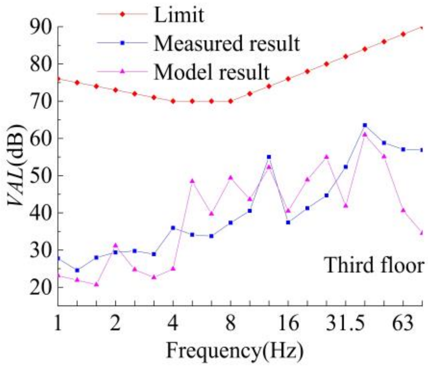

(c) Third floor

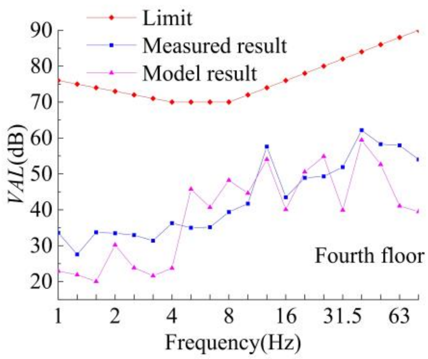

(d) Fourth floor

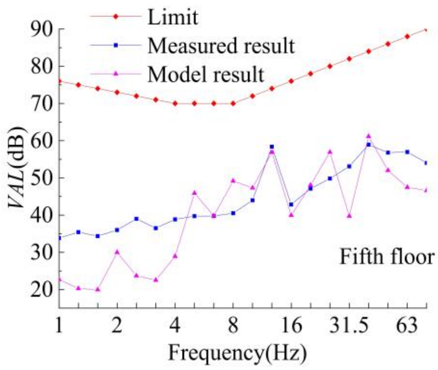

(e) Fifth floor

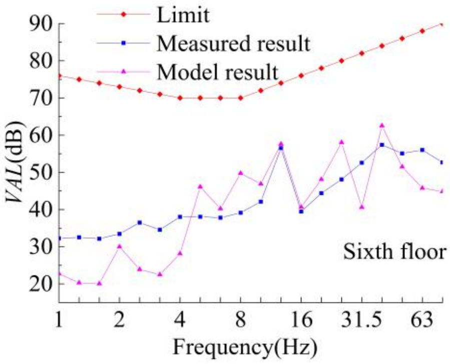

(f) Sixth floor

Fig. 14 Vibration acceleration level analysis of one-third octave frequency

limits specified in the code, it indicates that the No.1 building of the National Science Park of South China University of Technology meets the comfort requirements for work and residence.

It is no doubt that there exists difference between measured data and model data. In the model, the system is established based on various simplifications and assumptions. However, the factors affecting vibration response in the actual measurement are numerous and complicated, such as the influence of other transportation, the more complicated contact between each part of the structure and the difference between the actual building and the ideal model. What's more, ignoring the track unevenness also reduces the response (Kouroussis *et al.* 2015). But it should be emphasized that the accuracy requirements of this practical model have met the requirements of engineering applications.

5. Conclusions

This study builds a train-tunnel-soil-building model through the FEM software MIDAS GTS NX of the No.1 building of the National Science Park of South China University of Technology, which is built above line 3 of Guangzhou metro, then conducts on-site measurement to verify the model. Both data are used to analyze the influence of the subway induced vibration. The corresponding assumptions and conclusions in the paper are based on this frame structure. The following conclusions can be drawn from this study:

- The acceleration shows a tendency to decay with an increase of the floor, while the acceleration mainly concentrates in the range of $\pm$ 0.003 m/s^2.
- The frequency of the vibration is mainly concentrated at 30-80 Hz, while the amplitude frequency is

mainly concentrated at 30-50 Hz. The main component of vibration frequency does not change with an increase of the floor.

• The one-third octave vibration acceleration level curve shows the trend to increase first and then decrease, wherein the maximum value (64 dB) is obtained near 40 Hz.

• The vibration response of the model is in good agreement with the measured one, proving the correctness and applicability of the train-tunnel-soil-structure simulation method on serviceability assessment of subway induced vibration.

• The No.1 building can meet the requirements of work and residence comfort.

Acknowledgments

The research described in this paper was supported by the State Kay Laboratory of Subtropical Building Science (No. 2019ZB25). The writers would like to greatly acknowledge this financial support and express the most sincere gratitude.

References

Feng, S.J., Li, Y.C., Chen, Z.L. and Chen, H.X. (2017), "Response of railway track coupled with a stratified ground consisting of saturated interlayer to high-speed moving train load", *Soil Dynam. Earthq. Eng.*, **102**, 25-40. https://doi.org/10.1016/j.soildyn.2017.08.018.

He, C., Zhou, S.H., Guo, P.J. and Gong, Q.M. (2019), "Three-dimensional analytical model for the dynamic interaction of twin tunnels in a homogeneous half-space", *Acta Mechanica*, **230**(3), 1159-1179. https://doi.org/10.1007/s00707-018-2330-0.

dos Santos, N.C., Barbosa, J., Calcada, R. and Delgado, R. (2017), "Track-ground vibrations induced by railway traffic: experimental validation of a 3D numerical model", *Soil Dynam. Earthq. Eng.*, **97**, 324-344. https://doi.org/10.1016/j.soildyn.2017.03.004.

Feng, S.J., Zhang, X.L., Zheng, Q.T. and Wang, L. (2017), "Simulation and mitigation analysis of ground vibrations induced by high-speed train with three dimensional FEM", *Soil Dynam. Earthq. Eng.*, **118**, 66-73. https://doi.org/10.1016/j.soildyn.2017.01.022.

Jin, Q.Y., Thompson, D.J., Lurcock, D.E.J., Toward, M.G.R. and Ntotsios, E. (2018), "A 2.5D finite element and boundary element model for the ground vibration from trains in tunnels and validation using measurement data", *J. Sound Vib.*, **422**, 373-389. https://doi.org/10.1016/j.jsv.2018.02.019.

Yang, J.P., Li, P.Z. and Lu, Z. (2018), "Numerical simulation and in-situ measurement of ground-borne vibration due to subway system", *Sustainability*, **10**(7), 2439. https://doi.org/10.3390/su10072439.

Connolly, D.P., Kouroussis, G., Laghrouche, O., Ho, C.L. and Forde, M.C. (2015), "Benchmarking railway vibrations-Track, vehicle, ground and building effects", *Construct. Build. Mater.*, **92**, 64-81. https://doi.org/10.1016/j.conbuildmat.2014.07.042.

Lopes, P., Ruiz, J.F., Costa, P.A., Rodriguez, L.M. and Cardoso, A.S. (2016), "Vibrations inside buildings due to subway railway traffic. Experimental validation of a comprehensive prediction model", *Sci. Total Environ.*, **568**, 1333-1343. https://doi.org/10.1016/j.scitotenv.2015.11.016.

Lopez-Mendoza, D., Romero, A., Connolly, D.P. and Galvin, P. (2017), "Scoping assessment of building vibration induced by railway traffic", *Soil Dynam. Earthq. Eng.*, **93**, 147-161. https://doi.org/10.1016/j.soildyn.2016.12.008.

Kuo, K.A., Papadopoulos, M., Lombaert, G. and Degrande, G. (2019), "The coupling loss of a building subject to railway induced vibrations: Numerical modelling and experimental measurements", *J. Sound Vib.*, **442**, 459-481. https://doi.org/10.1016/j.jsv.2018.10.048.

Bian, X.C., Jiang, H.G., Chang, C., Hu, J. and Chen, Y.M. (2015), "Track and ground vibrations generated by high-speed train running on ballastless railway with excitation of vertical track irregularities", *Soil Dynam. Earthq. Eng.*, **76**, 29-43. https://doi.org/10.1016/j.soildyn.2015.02.009.

Yang, W.G., Wang, M., Shi, J.Q., Ge, J.Q., Zhang, N. and Ma, B.T. (2015), "Performance study on the whole vibration process of a museum induced by metro", *Struct. Eng. Mech.*, **55**(2), 413-434. http://dx.doi.org/10.12989/sem.2015.55.2.413.

Kouroussis, G., Florentin, J. and Verlinden, O. (2016), "Ground vibrations induced by intercity/interregion trains: a numerical prediction based on the multibody/finite element modeling approach", *J. Vib. Control*, **22**(20), 4192-4210. https://doi.org/10.1177/1077546315573914.

Zou, C., Wang, Y.M., Wang, P. and Guo, J.X. (2015), "Measurement of ground and nearby building vibration and noise induced by trains in a metro depot", *Sci. Total Environ.*, **536**, 761-773. https://doi.org/10.1016/j.scitotenv.2015.07.123.

Zou, C., Wang, Y.M., Moore, J.A. and Sanayei, M. (2017), "Train-induced field vibration measurements of ground and over-track buildings", *Sci. Total Environ.*, **575**, 1339-1351. https://doi.org/10.1016/j.scitotenv.2016.09.216.

Zou, C., Moore, J.A., Sanayei, M. and Wang, Y.M. (2018), "Impedance model for estimating train-induced building vibrations", *Eng. Struct.*, **172**, 739-750. https://doi.org/10.1016/j.engstruct.2018.06.032.

GB/T 50355-2005 (2005), "Standard of limit and measurement method of vibration in the room of residential buildings", Ministry of Housing and Urban–Rural Development of the Peoples' Republic of China; Beijing, China.

Auersch, L. (2005), "The excitation of ground vibration by rail traffic: theory of vehicle-track-soil interaction and measurements on high-speed lines", *J. Sound Vib.*, **284**(1-2), 103-132. https://doi.org/10.1016/j.jsv.2004.06.017.

Shibata A. and Sozen M.A. (1976), "Substitute structure method for seismic design in R/C", *J. Struct. Division*, **102**(1), 1-18.

Lai, J.X., Wang, K.Y., Qiu, J.L., Niu, F.Y., Wang, J.B. and Chen, J.X. (2016), "Vibration response characteristics of the cross tunnel structure", *Shock Vib.*, http://dx.doi.org/10.1155/2016/9524206.

Ling, Y.H., Wu, J.Z. and Ma, H.W. (2015), "Effects of subway vibration on a frame structure and its vibration isolation", *J. Vib. Shock*, **34**(4), 184-189.

Li, Q.T., Luo, Y. and Liu, Y. (2016), "Experimental research on identification of ground-borne noise from subway lines based on partial coherence analysis", *Proceedings of the 12th International Conference on Vibration Problems (ICOVP)*, Guwahati, India, December.

Kouroussis, G., Connolly, D.P., Alexandrou, G. and Vogiaztzis, K. (2015), "Railway ground vibrations induced by wheel and rail singular defects", *Vehicle Syst. Dynam.*, **53**(10), 1500-1519. https://doi.org/10.1080/00423114.2015.1062116.

CC